Catalysis Today 148 (2009) 124–129

Contents lists available at ScienceDirect

Catalysis Today

journal homepage: www.elsevier.com/locate/cattod

Selective production of hydrogen from partial oxidation of methanol over supported silver catalysts prepared by method of redox coprecipitation

Liuye Mo [a,c], Albert H. Wan [a], Xiaoming Zheng [c], Chuin-Tih Yeh [a,b,*]

[a] Department of Chemistry, National Tsinghua University, Hsinchu, Taiwan
[b] Fuel Cell Center, Yuan Ze University, Taoyuan, Taiwan 320
[c] Institute of Catalysis, Zhejiang University, Key Lab of Applied Chemistry of Zhejiang Province, Hangzhou 310028, China

ARTICLE INFO

Article history:
Available online 4 September 2009

Keywords:
Method of redox coprecipitation
Silver catalysts
Hydrogen production
Partial oxidation of methanol

ABSTRACT

Supported silver catalysts showed good activity for hydrogen production from partial oxidation of methanol (POM) at a low temperature of 160 °C. Ag/CeO_2–ZnO catalysts, prepared by the method of redox coprecipitation, displayed distinguished hydrogen selectivity (S_{H_2}) and methanol conversion. In preparation of the catalysts, Ag^+ ions were found reduced into metal clusters by Ce^{3+} ions. X-ray diffraction study revealed that the active silver crystallites were dispersed amorphously on the catalysts. Thermal characterization of temperature programmed hydrogen reduction and temperature programmed hydrogen desorption further suggested that CeO_2 and ZnO played different roles in the high S_{H_2} over Ag/CeO_2–ZnO. Promoter CeO_2 served as a spillover sink to collect hydrogen dissociated on silver crystallites while ZnO acted as a porthole for a fast desorption of hydrogen from the catalyst. These two oxides corporately raised the high S_{H_2} over Ag/CeO_2–ZnO catalysts.

1. Introduction

The proton exchanged membrane fuel cell (PEMFC) is an electric power with low pollution [1]. However, its application is hindered by difficulties in storage, transportation and distribution of hydrogen fuel. The difficulties may be relieved by on-site production of hydrogen from reforming liquid fuels. Methanol is regarded as a good fuel candidate for its ease handling, low cost, high energy density as well as commercialized as an important chemical feedstock [2].

Many methanol reforming reactions, i.e., steam reforming (SRM) [3,4], partial oxidation (POM) [5–9] and oxidative steam reforming (OSRM) [10,11] have been suggested to produce hydrogen from methanol. The endothermic SRM is an industrial process catalyzed by Cu/ZnO–Al_2O_3 at a reaction temperature of $T_o > 230$ °C. The exothermic POM used oxygen (air) as the oxidant:

$$CH_3OH + (1/2)O_2 \rightarrow 2H_2 + CO_2, \qquad \Delta H^\circ = -192.2\ \mathrm{kJ\,mol^{-1}} \tag{1}$$

In literature, POM reaction has been catalyzed by copper [5–7] and palladium [8,9] based catalysts. $T_o > 200$ °C was generally required for a high methanol conversion (C_{MeOH}). Besides the aimed product of H_2 and CO_2, side products of CO and H_2O were additionally formed. The selectivity of hydrogen (S_{H_2}) and carbon monoxide (S_{CO}) varied with the kind of metal and support. In our laboratory, a noble metal catalyst of Au/ZnO [12] displayed the highest S_{H_2} (~95%) and the lowest S_{CO} (<1%) for all the catalysts studied.

Silver crystallites dispersed on ZnO, Al_2O_3 and ZnO–Al_2O_3 were recently found to be active towards POM at $T < 160$ °C [13]. Unfortunately, observed S_{H_2} was poor (<60%) for hydrogen production from silver crystallites dispersed on monotony oxide. In a recent communication [14], we reported that good S_{H_2} (>90%) might be obtained from CeO_2 modified Ag/ZnO (Ag/Ce_{20}Zn catalyst in Table 1). Physical properties of the promoted catalysts have been subsequently characterized in the laboratory. In this report, we want to report our knowledge on the function of ZnO and the promotion of CeO_2 over Ag/CeO_2–ZnO catalysts to S_{H_2} of POM.

2. Experimental

2.1. Catalysts preparation

Supported silver catalysts of Ag/ZnO and Ag/CeO_2–ZnO were homely prepared. Cations in solutions of 0.15 M $AgNO_3$

* Corresponding author at: Fuel Cell Center, Yuan Ze University, Chongli, Taoyuan, Taiwan.
E-mail address: ctyeh@saturn.yzu.edu.tw (C.-T. Yeh).

0920-5861/$ – see front matter © 2009 Published by Elsevier B.V.
doi:10.1016/j.cattod.2009.04.002

Table 1
Effect of support on silver catalysts on POM performance at 160 °C.

Catalyst	C_{MeOH}	S_{H_2}	S_{CO_2}	S_{CO}
Ag/Al_2O_3[a]	67	5	92	8
Ag/ZnO	74	83	95	5
Ag/CeO_2	69	65	58	42
Ag/CeO_2 + quartz	54	24	89	11
Ag/CeO_2 + ZnO	78	88	98	2
$Ag/Ce_{0.6}Zn$	80	90	94	6
Ag/Ce_5Zn	83	91	95	5
$Ag/Ce_{20}Zn$	92	97	94	6
CeO_2/ZnO	0	–	–	–

[a] Data from Ref. [13].

(Riedel-dehaën) or a mixture solution of 0.15 M $AgNO_3$ and 0.40 M $Ce(NO_3)_3{\cdot}6H_2O$ (Riedel-dehaën) was adsorbed onto powders of ZnO ($d \sim 180$ nm, Merck) suspended in de-ionized water. Acidity of suspended solutions was subsequently adjusted to pH ~ 9.0 with 0.10 M NaOH. After stirring for 2 h at room temperature, the suspension was filtered, washed with de-ionized water and dried for 24 h at 100 °C as fresh catalysts. Fresh Ag/CeO_2 was prepared by the similar procedure without addition of ZnO. Ceria promoted Ag/CeO_2–ZnO samples of different CeO_2 content were designated as Ag/Ce_xZn (x represents nominal loading of Ce in wt.% of catalysts). The nominal loading of Ag was 5 wt.% in all of the prepared catalysts. True loadings of Ag in different catalysts were analyzed by ICP-MS and listed in the 2nd column of Table 2. Mixed samples of "Ag/CeO_2 + ZnO" and "Ag/CeO_2 + quartz" were prepared by physically mixing the Ag/CeO_2 with powders of ZnO and quartz sand at a ratio of 1:2, respectively. These mixtures were ground into fine powders, pressure-molded into granules, crushed again, sieved to 60–80 mesh and reduced at 200 °C for 1 h in a hydrogen flow, before used for activity tests.

2.2. Characterization

Temperature programmed reduction (TPR) studies were performed in a fixed bed apparatus described in a previous report [15]. A flow of 10 vol.% H_2/N_2 was used as carrier gas. Its flow rate was controlled to 30 ml/min by a mass flow controller. The sample temperature was linearly raised from room temperature to 700 °C at a rate of β = 7 °C/min. The amount of hydrogen consumption during sample reductions was monitored by a thermal conductivity detector (TCD).

Hydrogen temperature programmed desorption (H_2-TPD) was controlled by a quadrupole mass spectrometer (Omnistar™). Used catalyst (after 6 h reaction on stream) of 0.1 g was pretreated in a 10%H_2/Ar flow for 1 h at 160 °C and cooled down in the flow to ambient temperature (~25 °C). After purging with Ar for 0.5 h, H_2-TPD was controlled from room temperature to 700 °C with a ramp of 7 °C/min in the Ar flow.

X-ray powder diffraction (XRD) spectroscopy was recorded (MXP18 of MAC Science) with Cu Kα (λ = 1.540 Å) radiation. Reduced samples were mounted on sample holders and isolated by paraffin. Particle size of Ag crystallites dispersed on the catalysts was estimated by the Scherrer equation.

Table 2
Assignments of TPR for different catalysts and particle size of Ag over different catalysts.

Sample	Wt.% (Ag)	T_r (°C)			d_{Ag} (nm)
		Ag_2O	O_{ads}	Ce=O	
Ag_2O	N.D.	130	N.D.	N.D.	N.D.
Ag/ZnO	4.1	130	N.D.	N.D.	30
$Ag/Ce_{0.6}Zn$	3.5	130	190	N.D.	30
$Ag/Ce_{20}Zn$	4.8	N.D.	190	470	10
$Ce_{20}ZnO$	N.D.	N.D.	380	500	N.D.
Ag/CeO_2	3.9	N.D.	110–180	490	10
CeO_2	N.D.	N.D.	360–395	500	N.D.

N.D.: Not detected.

2.3. Catalytic reaction

Catalytic activity of prepared catalysts for POM reaction was tested in a fixed bed reactor (4 mm in id). A 100 ml/min flow of reactant gas ($n_{O_2}/n_{MeOH} = 0.5$) with 12.2 mol% CH_3OH (metered by a liquid pump and preheated to about 100 °C) and 6.1 mol% O_2 and 81.7 mol% Ar (controlled by mass flow controller) was catalyzed by 0.1 g reduced catalyst. Reaction products were analyzed by a GC equipped with TCD and columns of Porapak Q and Molecular Sieve 5A. Conversion of methanol (C_{MeOH}) and selectivity of H_2, CO_2 and CO were calculated according to the following equations:

$$C_{MeOH} = (n_{MeOH,in} - n_{MeOH,out})/n_{MeOH,in} \times 100\%;$$
$$S_{H_2} = n_{H_2}/(n_{H_2} + n_{H_2O}) \times 100\%;$$
$$S_{CO_2} = n_{CO_2}/(n_{CO_2} + n_{CO}) \times 100\%;$$
$$S_{CO} = n_{CO}/(n_{CO_2} + n_{CO}) \times 100\%.$$

3. Results

3.1. Phenomena of redox coprecipitation in catalyst preparation

Both of mono-salt $AgNO_3$ and $Ce(NO_3)_3$ aqueous solutions are transparent and colorless. However, tan and white precipitates were formed respectively by adding the NaOH solutions as given as follows:

$$2Ag^+ + OH^- = Ag_2O\downarrow \text{ (tan)} \quad (2)$$

$$Ce^{3+} + 3OH^- = Ce(OH)_3\downarrow \text{ (white)} \quad (3)$$

The precipitate of $Ce(OH)_3$ tended to be partially dehydrated and oxidized to yellow CeO_2 (nominated as fresh CeO_2 because of XRD characterization) upon a drying pretreatment at 100 °C [16]:

$$2Ce(OH)_3 + O_2 \rightarrow 2CeO_2 + 3H_2O \quad (4)$$

The structure of fresh CeO_2 must have contained a lot of adsorbed oxygen ($\equiv CeO_{ads}$). The O_{ads} is unstable and tends to be reduced by hydrogen [17,18] and CO [19,20]. However, O_{ads} may be relaxed and converted into stable lattice oxygen (capping and bridged) of CeO_2 upon thermal treatment at elevated temperatures. The extent of conversion increases with the treatment temperature.

Black precipitates, instead of the expected tan color, were formed as a bi-salt solution of $AgNO_3$ and $Ce(NO_3)_3$ was co-precipitated by the NaOH. The black color reflected fine crystallites of metallic Ag reduced by Ce^{3+} in the solution:

$$Ag^+ + Ce^{3+} + 4OH^- = Ag\downarrow \text{ (black)} + Ce(OH)_4\downarrow \quad (5)$$

The precipitation process in reaction (5) may be regarded as a "redox coprecipitation". The redox indicates a combination of the oxidation of Ce^{3+} ions into $Ce(OH)_4$ and the reduction of Ag^+ into metallic silver.

3.2. Temperature programmed reduction by hydrogen

Fig. 1 compares TPR traces for 0.1 g samples of commercial ZnO, commercial CeO_2, fresh CeO_2 and fresh $Ce_{20}Zn$ (20 wt.% of Ce deposited on commercial ZnO by precipitation with the same preparation procedure of Ag/Ce_xZn). The commercial ZnO was inert to hydrogen reduction and did not show any reduction peak up to 700 °C. The commercial CeO_2 (from Merck) showed a minor

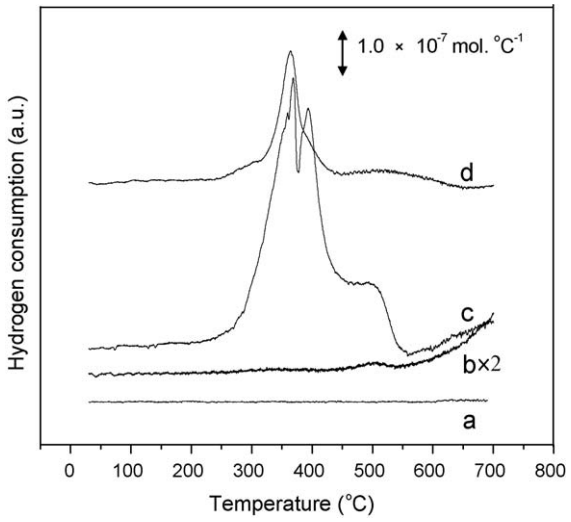

Fig. 1. TPR profiles of (a) ZnO, (b) commercial CeO_2, (c) CeO_2 and (d) $Ce_{20}Zn$ supports.

reduction at 500 °C and a prominent reduction upon 550 °C. The peak with 500 °C has been generally assigned to the reduction of Ce^{4+} attached with a capping oxygen (=Ce=O) on CeO_2 [18].

The high temperature peak at $T_r > 550$ °C reflects a reduction of bulk oxygen in the CeO_2 structure. In addition to the two peaks of commercial CeO_2, the fresh CeO_2 displayed an additional split peak at T_r = 360–395 °C. The peak may be attributed to a reduction of active O_{ads} (adsorbed during the drying at 100 °C). The splitting feature of this peak indicates a complex nature of the reduction. An extensive study is required for its resolution.

The peak caused by reduction of adsorbed oxygen was retained in the trace of $Ce_{20}Zn$ in Fig. 1. However, area of the peak was considerably reduced because of the decrease in the content of CeO_2. Yao and Yao Yu [18] also observed a reduction peak at $T_r \sim 400$ °C from a prereduced and reoxidized CeO_2/Al_2O_3 samples.

Fig. 2 compares TPR profiles of silver samples. Unsupported silver oxide showed a reduction peak at T_r = 130 °C. A peak with similar T_r appeared also in the TPR trace of freshly prepared Ag/ZnO (Fig. 2). The area of this peak suggests hydrogen consumption (n_{H_2}/n_{Ag}) of C_H = 0.47 which is in good agreement with the stoichiometry of the following reaction:

$$Ag_2O + H_2 \rightarrow 2Ag + 2H_2O \quad (6)$$

A prominently split peak maximized at T_r = 110 and 180 °C and a minor peak at T_r = 490 °C were observed from TPR profile of fresh Ag/CeO_2 in Fig. 2. Although the T_r range of the split peak covers T_r of Ag_2O (130 °C), the black color of this fresh sample suggests that deposited silver ions had already been reduced to metallic Ag (by reaction (5)) during preparation. Furthermore, the area of the split peak is very similar to the peak at 360–395 °C of CeO_2 in Fig. 1. The split peak in TPR trace of fresh Ag/CeO_2 may thus be attributed to reduction of active O_{ads} by spillover of hydrogen from Ag. Interestingly, the peak at 500 °C of CeO_2 was not significantly affected by the presence of Ag in Ag/CeO_2. Probably, reduction of capping oxygen cannot be effectively promoted by spillover.

Fig. 3 compares TPR trace of Ag/ZnO with those of Ag/Ce_xZn of different x ratios. Reduction of Ag_2O dispersed on Ag/ZnO was found at T_r = 130 °C. The intensity of this reduction peak decreased significantly on $Ag/Ce_{0.6}Zn$, became a shoulder to a peak of ~190 °C on Ag/Ce_5Zn catalyst, and disappeared completely as $x > 5$. Variation in the area of 130 °C peak in this figure confirms the former proposal that Ag^+ ions on fresh Ag/Ce_xZn catalysts had been reduced to metallic Ag by Ce^{3+} added in the preparation. The intended Ag loading in Ag/Ce_xZn catalysts was 5 wt.%. According to the stoichiometry of reaction (5), an x = 6.5 is required for a complete reduction of Ag^+ dispersed.

Besides the peak at T_r = 130 °C, two additional peaks at 190 and 470 °C were found in TPR traces of Ag/Ce_xZn. Their peak areas increased with the stoichiometry x. Similarly to the fresh CeO_2 (Fig. 1), the peak at 190 °C may be attributed to reduction of O_{ads} on CeO_2. The shift in T_r (see Table 2) strongly suggests that hydrogen is easily spillover from Ag to CeO_2 on Ag/Ce_xZn.

3.3. X-ray diffraction

Fig. 4 compares XRD profiles from fresh samples of Ag/ZnO, $Ag/Ce_{20}Zn$, $Ce_{20}ZnO$ and the reduced Ag/ZnO. Fresh Ag/ZnO showed two peaks distinctive for Ag_2O with 2(at ~32.8 and ~34.2°. The fresh $Ag/Ce_{20}Zn$ catalyst showed a weak peak at ~38.1° which is characteristic to (1 1 1) diffraction of metallic silver. The appearance of this peak further confirmed the TPR speculation that silver dispersed on the fresh $Ag/Ce_{20}Zn$ had already been reduced to metallic state by the redox reaction (reaction (5)) in preparation.

The Ag(1 1 1) peak has been used to examine the relative particle size of silver on Ag/Ce_xZn fully reduced by hydrogen at a temperature of 200 °C. The Scherrer equation has been used to estimate particle size (d_{Ag}) from peak width. Fig. 5 correlates variation of the particle

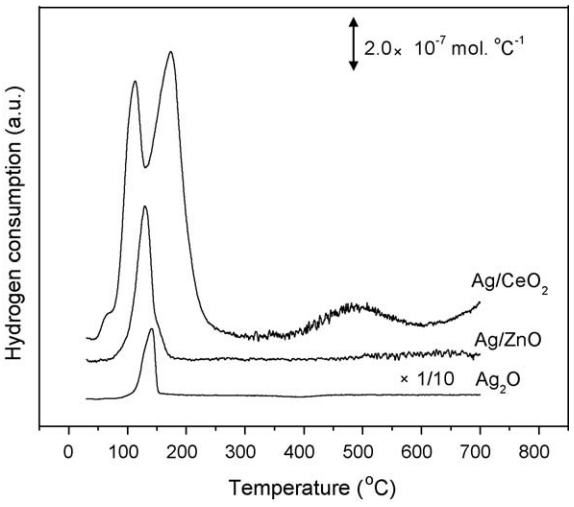

Fig. 2. TPR profiles of Ag_2O, Ag/ZnO and Ag/CeO_2 catalysts.

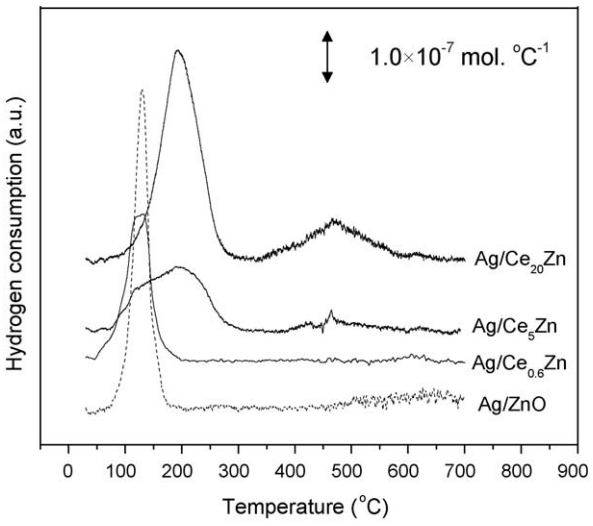

Fig. 3. Comparison of TPR profiles from fresh Ag/Ce_xZn.

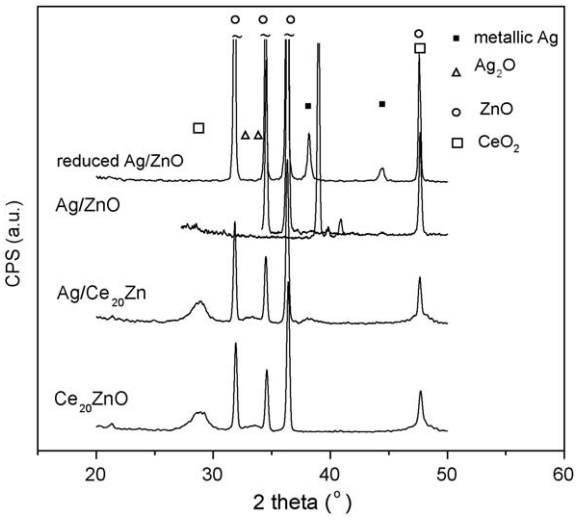

Fig. 4. XRD patterns of fresh samples of $Ag/Ce_{20}Zn$, Ag/ZnO and $Ce_{20}Zn$ and the reduced Ag/ZnO.

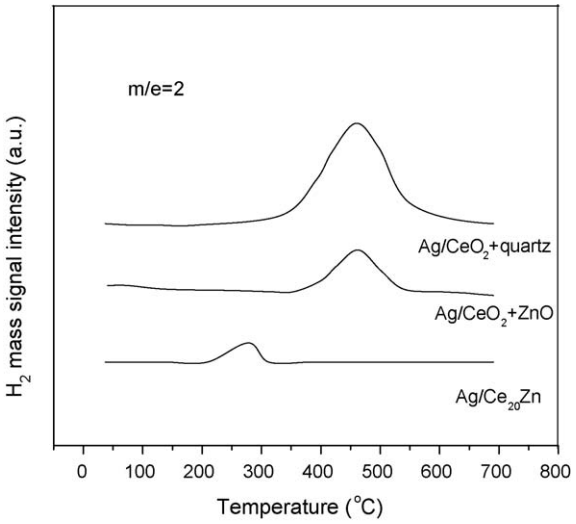

Fig. 6. H_2-TPD profiles from used catalyst of $Ag/Ce_{20}Zn$, Ag/CeO_2 + ZnO and Ag/CeO_2 + quartz.

size estimated with the stoichiometry x. Estimated d_{Ag} decreased substantially from 30 to 12 nm on increasing x from 0 to 5 and reached a plain of d_{Ag} = 10 nm as $x \geq 10$.

It is well known that XRD is insensitive to examine amorphous samples and small crystallites with a diameter of $d < 5$ nm. The peak area of XRD thus may be used to estimate the amount of crystallites with large d. Since the silver content of all the silver catalysts prepared in this study was similar (~5 wt.%, see Table 2), Ag(1 1 1) peak of their reduced samples should have a same area if all crystallites of Ag had a diameter of $d > 5$ nm. To the contrary, area of the peak of Ag(1 1 1) in samples of hydrogen reduced Ag/Ce_xZn varied with x. Ag/ZnO exhibited the largest peak area (Fig. 4). The area of this sample was therefore used as a reference to estimate the relative peak area (R_A) for samples of Ag/Ce_xZn. Fig. 5 indicates that R_A decreased with the stoichiometry x and lowered to 30% at $x \geq 10$. These results suggest that a large fraction of metallic Ag particles in highly promoted samples had a $d < 5$ nm and could not be detected by XRD. It is a pity that TEM technique also failed to characterize the size of Ag in our samples because the background of ZnO and CeO_2 was too dark.

3.4. H_2-TPD results

Partially reduced ceria was found to be capable of storing hydrogen [21,22]. Amount of hydrogen stored in used catalysts of $Ag/Ce_{20}Zn$, Ag/CeO_2 + ZnO and Ag/CeO_2 + quartz were examined by TPD studies. A same weight of Ag/CeO_2 was used in the physically mixed samples to compare their storage capacity. Ag/CeO_2 diluted with inert quartz was used instead of Ag/CeO_2 for a fair comparison. Fig. 6 compares H_2-TPD profiles obtained from aged samples pretreated by hydrogen at 160 °C. Ag/CeO_2 + ZnO and Ag/CeO_2 + quartz showed a same peak at T_d = 470 °C. Peak area of the sample Ag/CeO_2 + ZnO, however, was smaller (by a ratio of 0.44) than that of the sample Ag/CeO_2 + quartz. Conceivably, the hydrogen storage capacity of Ag/CeO_2 decreased on contacting with ZnO. $Ag/Ce_{20}Zn$ displayed the smallest desorption peak (by a ratio of 0.12 to the area of Ag/CeO_2 + quartz) among samples in Fig. 6. The peak position was also lowered to T_d = 280 °C. The corporation of ZnO to Ag/CeO_2 ($Ag/Ce_{20}Zn$) must have reduced the activation energy for desorption of the stored hydrogen.

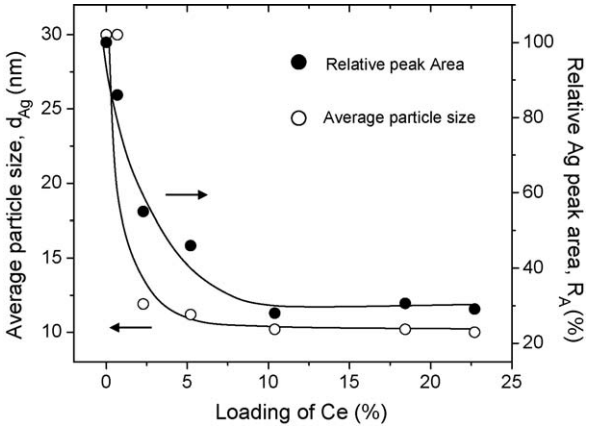

Fig. 5. Particle size of Ag and relative peak area vs. Ce loading over reduced Ag/Ce_xZn catalysts.

3.5. Catalytic performance

Table 1 gives the catalytic performance of the studied catalysts at 160 °C. Only H_2, H_2O, CO and CO_2 products were detected. The support of silver catalysts significantly affected the methanol conversion (C_{MeOH}) and product selectivity. Ag/ZnO showed a higher C_{MeOH} and the selectivity of intended products (S_{H_2} and S_{CO_2}) but a lower selectivity of the unwanted products (S_{CO} and S_{H_2O}) than Ag/CeO_2. However, the activity of Ag/CeO_2 mixing physically with ZnO (mixing catalyst of Ag/CeO_2 + ZnO) increased evidently. In order to exclude a possible dilute effect of ZnO in the mixing sample, a physical mixture of Ag/CeO_2 and quartz was also tried but showed poor catalytic performance.

Table 1 also indicates that an intimate incorporation of CeO_2 to Ag/ZnO in Ag/Ce_xZn may further promote S_{H_2} and C_{MeOH}. The promotion at 160 °C increased with the extent of incorporation. $Ag/Ce_{20}Zn$ exhibited the highest methanol conversion (C_{MeOH} = 92%) and S_{H_2} (97%) among the catalysts studied. Nevertheless, selectivities of CO_2 ($S_{CO_2} \sim 94\%$) and CO ($S_{CO} \sim 6\%$) were unaffected by the loading of Ce (x).

4. Discussions

4.1. Correlation between C_{MeOH} and S_{H_2}

Hydrogen and CO_2 were intended products of our POM reaction. High C_{MeOH}, S_{H_2} and S_{CO_2} are wanted at this study. Ag catalysts are generally active to POM at a low temperature of 160 °C. Table 1

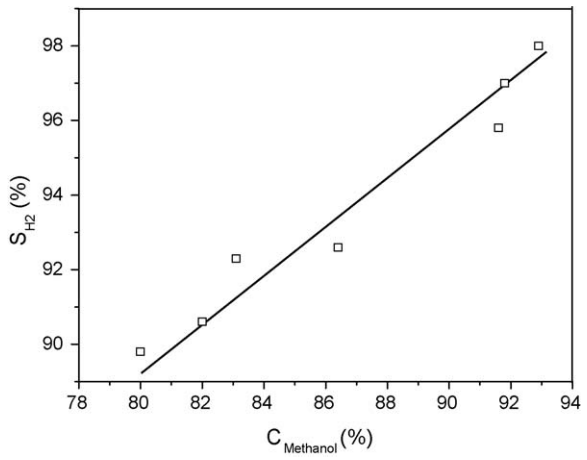

Fig. 7. Relationship between the conversion of methanol and the selectivity of H_2.

indicates that support of silver catalysts has a profound effect on C_{MeOH} and S_{H_2}. Ag/ZnO shows the highest C_{MeOH} and S_{H_2} among mono-oxide supported silver catalysts. CeO_2 is a good promoter to Ag/ZnO. Variation of POM activity at 160 °C over Ag/Ce_xZn catalysts was found from a formal report [14]. C_{MeOH} and S_{H_2} were found simultaneously increased with the stoichiometry *x*. A linear relationship between C_{MeOH} and S_{H_2} from POM over Ag/Ce_xZn catalysts is demonstrated in Fig. 7. The linearity may be qualitatively understood from the following facts:

1. The amount of oxygen supplied in reaction feed was in a fixed stoichiometry (~0.5) with that of MeOH.
2. Oxygen was fully consumed in POM reactions performed.
3. S_{CO_2} remained high (~94%) in the product.

High C_{MeOH} was therefore resulted in high S_{H_2} when a low fraction of O_2 was consumed for water formation.

4.2. Role of ZnO in POM reaction

The goal of this POM study is to produce hydrogen from reaction (1). Although silver catalysts are active, a portion of hydrogen decomposed from methanol was oxidized into water. A high selectivity to S_{H_2} is essential for the development of POM. Table 1 indicates that S_{H_2} of POM over silver catalysts prepared was significantly affected by their support. The following trend on S_{H_2} was noticed:

$$Ag/Ce_xZn > Ag/CeO_2 + ZnO > Ag/ZnO > Ag/CeO_2 > Ag/CeO_2 + quartz > Ag/Al_2O_3.$$

It is evident from this trend that ZnO is a good support for a high S_{H_2}.

ZnO support has been frequently regarded as good "porthole" to desorb di-hydrogen (H_2) [23]. In aromatization of light alkanes over catalysts, ZnO induced a removal of hydrogen species decomposed at acid site of zeolites [24]. In methanol decomposition or steam reforming of methanol over Cu/ZnO, ZnO also promoted desorption of hydrogen dissociated on metallic copper [25,26].

In TPD study of Fig. 6, hydrogen could be stored in used Ag/CeO_2 at the pretreatment stage. The area of TPD peak at 470 °C provides information on hydrogen storage capacity (HSC) of the used catalysts. The HSC of Ag/CeO_2 was found to significantly decrease (to a fraction of 0.44) by physically mixing with ZnO. Observed decrease in HSC may be attributed to a desorption of hydrogen through the porthole of ZnO at the reduction pretreatment. The effect of ZnO porthole becomes prominent in Fig. 6 for intimated contacted sample of $Ag/Ce_{20}Zn$. Not only HSC was dramatically deceased (to a fraction of 0.12), the stored hydrogen may be desorbed through ZnO at a low temperature of 280 °C.

4.3. Role of CeO_2

An incorporation of CeO_2 (Table 1) to Ag/ZnO promoted significantly its S_{H_2} of POM. The promotion of CeO_2 may be caused by two factors:

1. A fast sink for hydrogen from Ag crystallites: Figs. 2 and 3 indicate that Ag/CeO_2 and $Ag/Ce_{20}Zn$ have a big TPR peak at 190 °C. This peak has been assigned to spillover of hydrogen dissociated on silver to active inserted oxygen species on fresh CeO_2. TPD results of Fig. 6 have also demonstrated that the partially reduced CeO_2 exhibited significant capacity of hydrogen storage [21,22].
2. A reduction of d_{Ag} in catalysts: Fig. 5 indicates that Ag particles were significantly reduced as CeO_2 was added in Ag/Ce_xZn. Besides a spillover to the support, hydrogen dissociated on silver crystallites is also oxidized to water by oxygen adsorbed on the crystallites:

$$2H_{ad} + O_{ad} \rightarrow H_2O \quad (7)$$

A reduction in d_{Ag} definitely decreased the lifetime of hydrogen on silver and the chance of water formation from reaction (7). Accordingly, a high S_{H_2} was obtained.

The promotion role of CeO_2 may be described by a mechanism model depicted in Fig. 8. In order to simplify the model, the physical mixture catalyst of Ag/CeO_2 + ZnO was used as the model catalyst. It has been established that the rate-determining step of POM is the cleavage of the C–H bond of adsorbed methoxy group to form the surface-bond H_2CO species [27–34]. Over silver catalyst, the C–H bond on methoxy group is cleaved to form hydrogen atom with aid of silver.

Spillover of hydrogen from metal crystallites to support is difficult for Ag/Al_2O_3 but it is easy to occur reverse hydrogen spillover from Al_2O_3 surface to metal phase [35]. Hydrogen atoms (H_{ad}) on silver crystallites of these catalysts can either be oxidized to H_2O (reaction (7)) or desorbed as H_2. A $S_{H_2} < 10\%$ was therefore resulted from POM (see Table 1) over Ag/Al_2O_3. H_{ad} on Ag crystallites of Ag/CeO_2 may be reversibly spillover to the support (TPR results). The hydrogen spillover on CeO_2 tends to desorb as di-hydrogen rather than being oxidized to water and the selectivity of hydrogen was improved to S_{H_2} = 65% (Table 1). When porthole ZnO was physically mixed with Ag/CeO_2, the spillover hydrogen on CeO_2 could quickly desorbed as H_2 through the ZnO. In such case, S_{H_2} may be increased over 88% through a synergistic corporation between CeO_2 and ZnO.

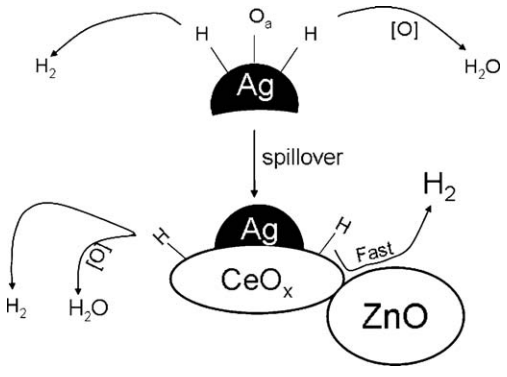

Fig. 8. Schematic of production of hydrogen from POM.

5. Conclusions

Ag/ZnO catalyst showed excellent catalytic activity for POM at low temperatures. A promotion of this catalyst with CeO_2 significantly increased C_{MeOH} and S_{H_2}. Following knowledge was concluded from the present TPR, TPD and XRD characterizations:

1. Ag^+ ions were reduced by Ce^{3+} (reaction (5)) during the preparation of Ag/Ce_xZn catalysts used in this study. This new preparation method is named as "redox coprecipitation".
2. The size of active Ag crystallites on Ag/Ce_xZn catalysts prepared by this method was small ($d_{Ag} < 5$ nm) and could not be detected by XRD.
3. Ceria and ZnO in Ag/Ce_xZn catalysts act as spillover sink to collect hydrogen decomposed on active silver and porthole for fast desorption of hydrogen from ceria, respectively. These two oxides synergistically promoted a high S_{H_2} from POM over Ag/Ce_xZn.

Acknowledgements

One of the authors, L.Y. Mo, appreciates the Minister of Education of the Republic of China for a post-doctoral fellowship. We thank the financial supports by National Science Foundation of China (20703035) and Zhejiang Province Science and Technology Department (2005E10016). We also thank the reviewers' beneficial suggestions on how to improve this manuscript.

References

[1] A.J. Appleby, F.R. Foulkes, Fuel Cell Handbook, Van Nostrand Reinhold, New York, 1989.
[2] W. Cheng, H.H. Kung, Methanol Production and Use, Marcel Dekker, New York, 1994.
[3] J.P. Breen, J.R.H. Ross, Catal. Today 51 (1999) 521.
[4] S. Ito, Y. Suwa, S. Kondo, S. Tameoka, K. Tomishige, K. Kumimori, Catal. Commun. 4 (2003) 499.
[5] T.J. Huang, S.W. Wang, Appl. Catal. 24 (1986) 287.
[6] Z.F. Wang, J.Y. Xi, W.P. Wang, G.X. Lu, J. Mol. Catal. A: Chem. 191 (2003) 123.
[7] L. Alejo, R. Lago, M.A. Peña, J.L.G. Fierro, Appl. Catal. A: Gen. 162 (1997) 281.
[8] J. Agrell, G. Germani, S.G. Jaras, M. Boutonnet, Appl. Catal. A: Gen. 242 (2003) 233.
[9] M.L. Cubeiro, J.L.G. Fierro, J. Catal. 179 (1998) 150.
[10] J.P. Shen, C.S. Song, Catal. Today 77 (2002) 89.
[11] S. Velu, K. Suzuki, M. Okazaki, M.P. Kapoor, T. Osaki, F. Ohashi, J. Catal. 194 (2000) 373.
[12] C. T. Yeh, Low Temperature Reforming Process for Production of Hydrogen from Methanol, US Patent 7459000 (2008).
[13] C.T. Yeh, Y.J. Chen, H.S. Hung, A Process of Producing Hydrogen under Low Temperature, Taiwan Patent I226308 (2005).
[14] L.Y. Mo, X.M. Zheng, C.T. Yeh, Chem. Commun. (2004) 1426.
[15] S. Yuvaraj, F.Y. Lin, T.H. Chang, C.T. Yeh, J. Phys. Chem. B 107 (2003) 1044.
[16] E. Abiaad, R. Bechara, J. Grimblot, A. Aboukais, Chem. Mater. 5 (1993) 793.
[17] C. Li, K. Domen, K. Maruya, T. Onishi, J. Am. Chem. Soc. 111 (1989) 7683.
[18] H.C. Yao, Y.F. Yao Yu, J. Catal. 86 (1984) 254.
[19] X. Zhang, K.J. Klabunde, Inorg. Chem. 31 (1992) 1706.
[20] V. Vladimir, I.K. Vladimir, L. Julie, J. Phys. Chem. B 108 (2004) 5341.
[21] L. Tournayan, N.R. Marcilio, R. Frety, Appl. Catal. 78 (1991) 31.
[22] S. Bernal, J.J. Calvino, G.A. Cifredo, J.M. Gatica, J.M. Omil, J.M. Pintado, J. Chem. Soc., Faraday Trans. 89 (1993) 3499.
[23] J.A. Biscardi, E. Iglesia, Catal. Today 31 (1996) 207.
[24] R.L.V. Mao, L. Dufresne, J.H. Yao, Appl. Catal. 65 (1990) 143.
[25] L. Chan, G.L. Griffin, Surf. Sci. 173 (1986) 160.
[26] R.O. Item, N.N. Bakhshi, Ind. Eng. Chem. Res. 34 (1995) 1548.
[27] B.A. Peppley, J.C. Amphlett, L.M. Kearns, R.F. Mann, Appl. Catal. A: Gen. 179 (1999) 21.
[28] B.A. Peppley, J.C. Amphlett, L.M. Kearns, R.F. Mann, Appl. Catal. A: Gen. 179 (1999) 31.
[29] M. Bowker, R.J. Madix, Surf. Sci. 95 (1980) 190.
[30] M. Mavrikakis, M.A. Barteau, J. Mol. Catal. A: Chem. 131 (1998) 135.
[31] C.J. Jiang, D.L. Trimm, M.S. Wainwright, N.W. Cant, Appl. Catal. A: Gen. 97 (1993) 145.
[32] G.J. Millar, C.H. Rochester, K.C. Waugh, J. Chem. Soc., Faraday Trans. 87 (1991) 2795.
[33] S.R. Bare, J.A. Stroscio, W. Ho, Surf. Sci. 150 (1985) 399.
[34] S.M. Gates, J.N. Russel, J.T. Yates, Surf. Sci. 159 (1985) 233.
[35] L. Huang, Y. Zhu, C. Huo, H. Zheng, G. Feng, C. Zhang, Y. Li, J. Mol. Catal. A: Chem. 288 (2008) 10.